First Liquid Layer Inertial Confinement Fusion Implosions at the National Ignition Facility

R. E. Olson,[1] R. J. Leeper,[1] J. L. Kline,[1] A. B. Zylstra,[1] S. A. Yi,[1] J. Biener,[2] T. Braun,[2] B. J. Kozioziemski,[2] J. D. Sater,[2] P. A. Bradley,[1] R. R. Peterson,[1] B. M. Haines,[1] L. Yin,[1] L. F. Berzak Hopkins,[2] N. B. Meezan,[2] C. Walters,[2] M. M. Biener,[2] C. Kong,[3] J. W. Crippen,[3] G. A. Kyrala,[1] R. C. Shah,[1] H. W. Herrmann,[1] D. C. Wilson,[1] A. V. Hamza,[2] A. Nikroo,[2] and S. H. Batha[1]

[1]*Los Alamos National Laboratory (LANL), Los Alamos, New Mexico 87185, USA*
[2]*Lawrence Livermore National Laboratory (LLNL), Livermore, California 94551, USA*
[3]*General Atomics (GA), San Diego, California 92186, USA*

(Received 22 August 2016; published 7 December 2016)

The first cryogenic deuterium and deuterium-tritium liquid layer implosions at the National Ignition Facility (NIF) demonstrate D_2 and DT layer inertial confinement fusion (ICF) implosions that can access a low-to-moderate hot-spot convergence ratio ($12 < CR < 25$). Previous ICF experiments at the NIF utilized high convergence ($CR > 30$) DT ice layer implosions. Although high CR is desirable in an idealized 1D sense, it amplifies the deleterious effects of asymmetries. To date, these asymmetries prevented the achievement of ignition at the NIF and are the major cause of simulation-experiment disagreement. In the initial liquid layer experiments, high neutron yields were achieved with CRs of 12–17, and the hot-spot formation is well understood, demonstrated by a good agreement between the experimental data and the radiation hydrodynamic simulations. These initial experiments open a new NIF experimental capability that provides an opportunity to explore the relationship between hot-spot convergence ratio and the robustness of hot-spot formation during ICF implosions.

DOI: 10.1103/PhysRevLett.117.245001

Thermonuclear ignition via indirect-drive inertial confinement fusion (ICF) is one of the primary goals of the U.S. Department of Energy research at the National Ignition Facility (NIF) [1]. The NIF is, by far, the largest and most powerful laser facility in the world. In indirect-drive ICF, the high power (~500 TW) NIF laser beams are used to heat the interior walls of a high-Z enclosure (or "hohlraum") to temperatures in the range of 270–300 eV. In the center of the hohlraum, there is a low-Z spherical shell (or "capsule") that contains a layer of cryogenic deuterium-tritium (DT) fuel. The x rays emitted by the hot, high-Z hohlraum walls are strongly absorbed by the capsule, rapidly ablating the low-Z capsule material. As this ablated material expands outward, the remaining capsule mass and enclosed DT fuel layer are accelerated inward by a spherical, ablation-driven rocket effect. When the shell converges on center, the kinetic energy is converted into a high-pressure fuel assembly. Conceptually, the imploded DT fuel assembly consists of a central hot spot surrounded by a shell of cold, very high density DT. The hot-spot convergence ratio is defined as the ratio of the initial inner radius of the DT layer, R_i, to the radius of the hot spot, R_{hs} (i.e., $CR = R_i/R_{hs}$). In order to achieve ignition and energy gain, the hot-spot temperature must be >4 keV—high enough for fusion product energy deposition to balance losses due to bremsstrahlung radiation. Provided the hot-spot areal density is sufficient (~0.3 gm/cm^2), α particles from T(D, n)α fusion reactions will further heat the hot spot, causing ignition and thermonuclear burn propagation into the surrounding cold fuel. The approach to ICF ignition at the NIF during the 2009–2012 National Ignition Campaign (NIC) employed high convergence ($CR > 30$) implosions using capsules containing a layer of DT ice [2]. The NIC experiments using the ice layer capsules with high CR implosions failed to achieve ignition, producing thermonuclear energy outputs that were 2–3 orders of magnitude below expectations based upon predictions of 1D radiation-hydrodynamic code simulations [3]. Although high CR is desirable in an idealized 1D sense, it amplifies the deleterious effects of realistic features, including x-ray drive asymmetries in the hohlraum, growth of instabilities seeded by capsule surface roughness, capsule defects, and the capsule fill tube and support hardware [4].

A typical NIC capsule has an inner radius of about 850 μm and contains a DT ice layer that is about 70 μm thick. The central volume contains DT vapor. Use of a DT ice layer requires the initial temperature of the capsule to be below the DT triple point temperature of 19 °K. Because of the low vapor density at temperatures below the triple point (a typical NIC ice layer capsule has a vapor density <0.4 mg/cm^3), the central volume does not contain enough mass to create a hot spot. At these low temperatures, a NIC capsule can contain only about 7% of the required hot-spot mass within the vapor. More than 90% of the hot-spot mass must be contributed, through inefficient heating mechanisms, from mass originally residing in a thin (~3 μm) layer at the inner surface of the DT ice [5]. In a

NIC capsule implosion, the compressed hot spot is typically about 25 μm in radius, with a hot-spot convergence ratio CR = 850/25 = 34. There are significant difficulties involved in uniformly and symmetrically shocking and heating the thin, inner portion of the ice layer to the high temperature required for the creation of an ignited hot spot. In addition, high CR implosions must address challenges involving sensitivities to small asymmetries in the x-ray drive flux combined with the effects of realistic three-dimensional features such as capsule support hardware and capsule fill tubes [4].

A recent theoretical study [5] suggests that the hot spot can be more efficiently formed with a reduced CR (CR < 20) by using a DT liquid layer with an increased initial DT vapor mass. A DT liquid layer allows for a much higher vapor density than is possible with a DT ice layer. The wide range of vapor densities that are possible with liquid layers having initial temperatures in the range of 20–26 °K provides flexibility in hot-spot CR (12 < CR < 25), which, in turn, will provide a reduced sensitivity to asymmetries and instability growth. Given enough vapor mass, the hot spot can be formed by sending a strong shock through the vapor, with the imploding cold, dense fuel layer further heating the hot plasma via a compression work (PdV) process. In this manner, the formation of the hot spot and the formation of the dense fuel layer are separated, and the hot-spot formation is simplified and more efficient compared to a traditional ice layer implosion. In this Letter, we present the first experimental results of a liquid DT layer implosion platform that can be used to scan a wide range of initial vapor densities and implosion CRs that can help to provide a fundamental understanding of the ICF hot-spot formation process.

The DT ice layer and the DT liquid layer ICF concepts have been discussed for more than 25 years. After many years of research, the β-layering technique [6] used to form a DT ice layer developed to the point where it is routinely used in ICF implosion experiments. The formation of a liquid layer requires a foam liner on the inner surface of the capsule [7]. It is only within the last few years that a target fabrication process developed for lining the interior of a NIF ICF capsule with an ultralow density CH foam that has the required uniformity and is robust enough to survive wetting with liquid hydrogen [8,9]. It is this new target fabrication innovation, together with the emergence of the NIF high density carbon (HDC) capsule and near-vacuum hohlraum (NVH) platform [10,11] that led to the recent liquid D_2 and liquid DT wetted foam layer experiments reported on in this Letter.

The experimental setup is illustrated in Fig. 1. Using the target fabrication process described in Refs. [8,9], a thin (~30 μm) low density (~50 mg/cm^3) CH foam layer is created on the inner surface of a HDC capsule. The capsule is then placed into the hohlraum. After the target is cooled to a temperature in the range of 20 °K to 26 °K, liquid D_2 or liquid DT flows into the capsule through a 30 μm diameter

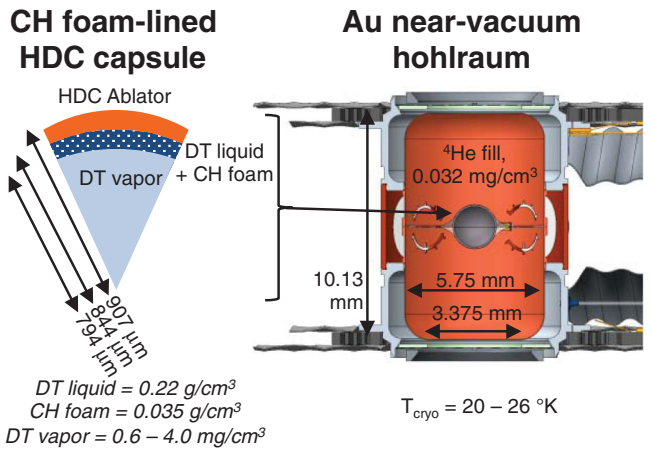

FIG. 1. Illustration of the capsule and hohlraum used in the liquid layer experiments. The HDC shell thickness is 63 μm, and the outer radius is 907 μm.

fill tube, saturating the CH foam layer. Control of the target temperature allows for the initial vapor density in the central region of the capsule to be set in the range of 0.6 mg/cm^3 (at 20 °K) to 4.0 mg/cm^3 (at 26 °K). By comparison, typical DT ice layer capsules (which must be below the DT triple point temperature of 19 °K) have a central region vapor density in the range of 0.3–0.4 mg/cm^3 (the maximum possible vapor density being 0.46 mg/cm^3), and it takes a long time (several days) to form a DT ice layer.

Our choice of laser pulse shape was based upon a preceding series of subscale experiments [12] employing a three-shock pulse shape with the type of gas-filled HDC capsules routinely used to tune the symmetry ("symcaps"). These symcap experiments used HDC capsules and NVHs with dimensions nearly identical to those shown in Fig. 1, except that the capsules did not have the liquid layer and were filled instead with high pressure DHe^3 gas. As explained in Ref. [12], a predictive capability was developed using the HYDRA radiation hydrodynamics code [13] in 2D integrated simulations (i.e., modeling the complete hohlraum and capsule setup with laser beam input) for designing a symmetric implosion with a CR ~ 12. For the liquid layer experiments, we used the Ref. [12] HYDRA model and modified the laser pulse in two important ways relative to the "round implosion" symcap pulse. First, 200 ps was added to the length of the "foot" of the pulse shape. This was done to ensure that the first two shocks would coalesce in the vapor and not in the liquid layer. Second, because of the longer foot, the inner and outer beam powers were altered in a time-resolved fashion ("dynamic beam phasing" [12]) relative to the symcap pulse shape in order to retain a symmetric implosion with the longer pulse shape (inner beams heat the central region of the hohlraum, while outer beams heat the upper and lower regions). The resulting laser pulse shape used in the

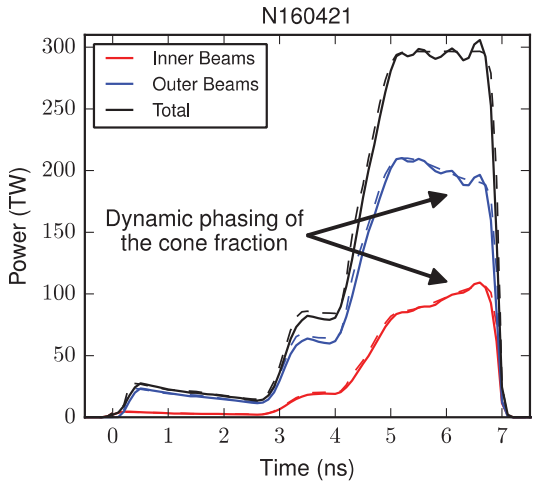

FIG. 2. The laser pulse shape used in the initial liquid layer experiments requires <900 kJ, less than half of the full NIF capability (the dashed curve is the requested pulse; the solid curve is the actual delivered pulse).

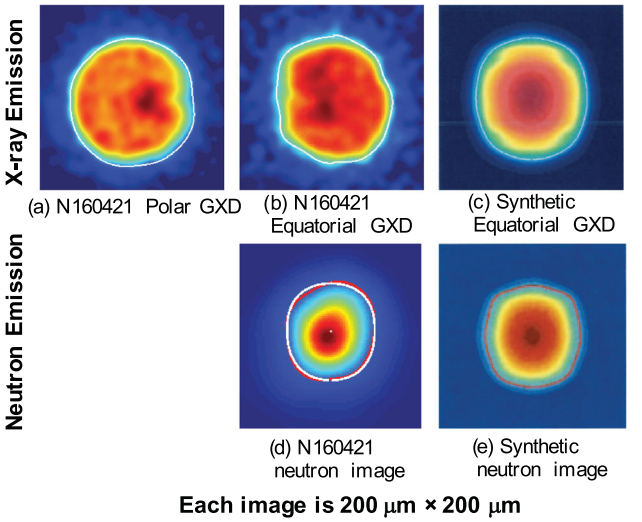

FIG. 3. (a) Polar x-ray image of a hot spot at bang time; (b) equatorial x-ray image; (c) synthetic x-ray image from the simulation; (d) neutron image of the hot spot; (e) synthetic neutron image from the simulation.

initial liquid D_2 and DT experiments is shown in Fig. 2. This laser pulse shape requires 869 kJ of laser energy (less than half of the full NIF laser capability) and utilizes very little of the NIF laser optics damage budget. In general, subscale experiments are being used at the NIF for the introduction of new physics platforms.

As can be seen in Fig. 3, the integrated HYDRA design techniques successfully produced a large, round hot spot in the first liquid DT layer implosion at the NIF. The polar x-ray image [14,15] [Fig. 3(a)] at bang time has a radius (M_0) of 68.8 ± 2.4 μm with a ratio of Legendre moments M_2/M_0 of $(1.8 \pm 1.1)\%$, and the equatorial x-ray image [Fig. 3(b)] indicates a hot spot with a radius (P_0) of 64.7 ± 4.7 μm with a ratio of Legendre moments P_2/P_0 of $(7.7 \pm 1.3)\%$. The primary neutron image [16] [Fig. 3(d)] shows a round, centrally peaked thermonuclear burning region with a radius of 50.6 ± 2.18 μm with a P_2/P_0 of 8%. An integrated, postshot 2D HYDRA simulation of this experiment was postprocessed to provide a synthetic equatorial x-ray image [Fig. 3(c)] and a primary neutron image [Fig. 3(e)]. For both of these hot-spot metrics, the synthetic images have radii and a shape that are within the uncertainty of the measurements. The observed and simulated thermonuclear burn histories [17] are compared in Fig. 4. The level of agreement, to within better than 15% in FWHM of burn width, is much better than typical for DT ice layer implosion experiments at the NIF.

A comparison of the observed and simulated values for a number of key performance metrics for the liquid DT layer experiment is given in Table I. Simulation results using both HYDRA [13] and RAGE [18] are included in the table. It can be seen that the simulations and measurements [19,20] of the burn-averaged DT ion temperature and the burn-averaged DD ion temperature are in agreement. This is an important feature of this DT liquid layer experiment. It is usually found in DT ice layer implosions that the measured DT ion temperature exceeds the expectation from simulations—an indication of inefficiency in hot-spot formation due to incomplete stagnation and residual kinetic energy effects [21]. The hot-spot pressures included in the table have been inferred in two ways from both the experimental and synthetic data. In one case, the experimental and synthetic x-ray images have been combined with experimental and simulation values of the DT ion temperature, burn history, and neutron yield to infer a hot-spot pressure (in a manner similar to Ref. [22]). In the other version, the experimental and synthetic primary neutron images are used instead of the x-ray images. For both versions, the hot-spot pressure inferred from the synthetic data is within the uncertainties of the hot-spot pressure inferred from the experimental data. The table includes experimental and

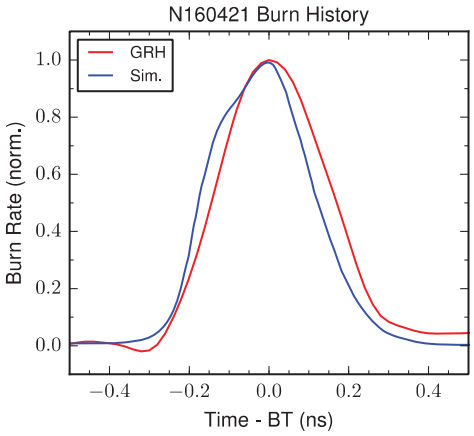

FIG. 4. Thermonuclear burn history measurement compared to burn history in the simulation. Time (ns) is in relation to bang time (BT).

TABLE I. N160421 implosion metrics.

	Data	2-D HYDRA	1-D RAGE	2-D RAGE
DT neutrons (10^{14})	4.5 ± 0.1	6.4	5.7	4.9
Nuclear bang time (ns)	8.49 ± 0.03	8.6	8.45	8.5
DT T_i (keV)	3.2 ± 0.1	3.3	3.3	3.3
DD T_i (keV)	3.0 ± 0.2	3.1	3.0	3.0
Nuclear burn width (ps)	313 ± 30	287	243	275
Hot-spot radius (μm) X-ray image	64.7 ± 4.7	61.8	65.4	65
Neutron image	50.6 ± 2.2	53	52	47
Inferred pressure (GBar) X-ray image	16.5 ± 2.6	18.5	17.3	17
Neutron image	23.5 ± 2.6	23.5	21.8	...

simulation values for the DT neutron yield. The neutron yield (or total number of 14.1 MeV neutrons) is a direct indication of the number of $\mathrm{T(D},n)\alpha$ fusion reactions occurring in the experiment. For the 2D integrated HYDRA and 1D RAGE simulations (the 1D RAGE simulations include a mix model [23]), the measured yield over calculated yield (YOC) varies from 70% to 80%. It should be noted that these first-of-a-kind, NIF subscale liquid hydrogen layer experiments utilized a larger than usual capsule fill tube. This was done to accommodate the CH foam layering process as described in Refs. [8,9]. The effect of the fill tube, together with the capsule's tent support membrane and surface roughness (for both the HDC ablator and wetted foam liquid layer), was included in the 2D RAGE simulation. This simulation, with YOC $> 90\%$, indicates that jetting of ablator material into the hot spot, caused by the capsule fill tube, degrades the DT neutron yield by about 15%.

Up to this point, our discussion of experimental results has concentrated on NIF shot N160421, which was the first liquid DT layer experiment. It should be noted that our very first liquid layer experiment, NIF shot N160320, was done with a liquid D_2 layer, with all other fielding parameters (including the initial cryogenic temperature) being identical to liquid DT layer shot N160421. The hot-spot size, with GXD $M0 = 62.0 \pm 1.3$ μm and $P0 = 63.6 \pm 2.8$ μm, was comparable to N160421 and the shape, with $M2/M0 = (12.3 \pm 1.2)\%$ and $P2/P0 = (-16.2 \pm 4.2)\%$, was not quite as round as N160421, principally due to issues involving the laser beams on that particular shot. Experiment N160320 is notable in that it represents the first implosion of a D_2 layered capsule of any kind at the NIF. The reduced neutron yield and relatively fast turnaround of a liquid D_2 layer implosion platform opens up the possibility for a variety of surrogate experiments that might be used in experimental studies of layered implosions with unprecedented flexibility in the hot-spot CR. Experiments using DT ice layers are more difficult and expensive for the facility, due to the use of tritium, yield stay-out time, and instrument damage from high neutron fluence. The new platform also enables designs in which dopants in the foam, and thus in the fuel layer, can be used to diagnose the plasma conditions at the edge of the hot spot, the density of the cold fuel surrounding the hot spot, and the mix of cold fuel into the hot spot.

Our third liquid layer experiment, NIF shot N160626, was designed to demonstrate that we could, in fact, increase the hot-spot CR. The success of this demonstration is illustrated in Figure 5. In comparing N160421 and N160626, the yield and symmetry were similar, and the key differences were (i) a reduction in hot-spot size (about 30% smaller), (ii) an increase in inferred hot-spot pressure (about 40% higher), and (iii) a reduction in thermonuclear burn width (about 30% narrower in FWHM). The burn duration is proportional to the hot-spot radius or sound speed and so is expected to decrease with an increasing CR.

In summary, we report the first cryogenic liquid layer capsule implosion experiments at the NIF. These are the first layered ICF implosions at the NIF in which the hot spot is formed from mass originating in the central vapor region of the capsule. The key diagnostic measurements made in the initial liquid DT layer experiment are well understood, based upon comparisons between the experimental data and the radiation hydrodynamic simulations. We demonstrate for the first time implosions of cryogenic DT layered capsules with a low hot-spot convergence ratio (CR < 20). These experiments demonstrate the ability to

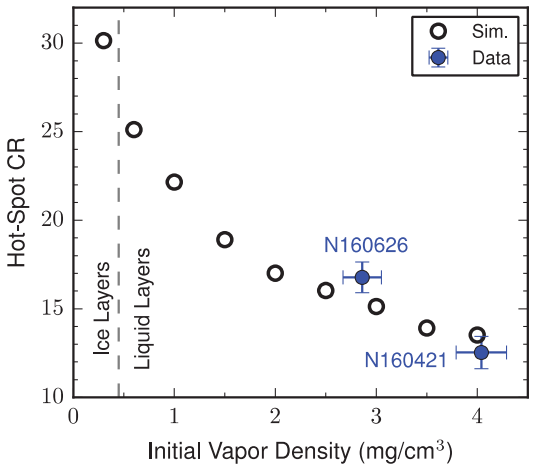

FIG. 5. The expected variation of the CR with vapor density (black circles) and our initial experimental results (blue squares).

vary the CR of a layered implosion in a predictable manner via a change in the initial cryogenic fielding temperature of the target. High neutron yields (comparable to many of the full laser energy NIC experiments) were achieved despite using less than half of the NIF laser energy. We also performed the first D_2 layer implosion at the NIF. These first liquid layer experiments create a new NIF experimental platform that provides an opportunity to explore the relationship between the hot-spot convergence ratio and the efficiency of hot-spot formation during ICF implosions. The new platform also enables designs in which dopants in the fuel layer can be used to diagnose the plasma conditions at the edge of the hot spot, the density of the cold fuel surrounding the hot spot, and the mix of cold fuel into the hot spot.

We thank S. Khan, T. Ma, R. Benedetti, and N. Izumi (LLNL) for the x-ray shape analysis; C. Yeamans, D. Sayre, and R. Hatarik (LLNL) and M. Gatu Johnson (MIT) for the neutron analysis; F. Merrill (LANL) for the neutron image analysis; N. Rice and H. Huang (GA) for capsule and foam layer characterization; and the NIF operations, laser, target fabrication, and diagnostic teams for their efforts during these experiments. This work was performed under the auspices of the U.S. Department of Energy by LANL under Contract No. DE-AC52-06NA25396, by LLNL under Contract No. DE-AC52-07NA27344, and by GA under Contract No. DE-NA0001808.

[1] E. Moses, R. N. Boyd, B. A. Remington, C. J. Keane, and R. Al-Ayat, Phys. Plasmas **16**, 041006 (2009).
[2] S. W. Haan *et al.* Phys. Plasmas **18**, 051001 (2011).
[3] J. D. Lindl *et al.*, Phys. Plasmas **21**, 129902 (2014).
[4] D. S. Clark *et al.*, Phys. Plasmas **23**, 056302 (2016).
[5] R. E. Olson and R. J. Leeper, Phys. Plasmas **20**, 092705 (2013).
[6] J. K. Hoffer and L. R. Foreman, Phys. Rev. Lett. **60**, 1310 (1988).
[7] R. A. Sacks and D. H. Darling, Nucl. Fusion **27**, 447 (1987).
[8] J. Biener *et al.*, Nucl. Fusion **52**, 062001 (2012).
[9] T. Braun, C. C. Walton, C. Dawedeit, M. M. Biener, S. H. Kim, T. M. Willey, X. Xiao, A. van Buuren, A. V. Hamza, and J. Biener, ACS Appl. Mater. Interfaces **8**, 2600 (2016).
[10] N. B. Meezan *et al.*, Phys. Plasmas **22**, 062703 (2015).
[11] S. Le Pape *et al.*, Phys. Plasmas **23**, 056311 (2016).
[12] L. F. Berzak Hopkins *et al.*, Phys. Plasmas **22**, 056318 (2015).
[13] M. M. Marinak, R. E. Tipton, O. L. Landen, T. J. Murphy, P. Amendt, S. W. Haan, S. P. Hatchett, C. J. Keane, R. McEachern, and R. Wallace, Phys. Plasmas **3**, 2070 (1996).
[14] G. A. Kyrala *et al.*, Rev. Sci. Instrum. **81**, 10E316 (2010).
[15] S. F. Khan *et al.*, Rev. Sci. Instrum. **83**, 10E118 (2012).
[16] F. E. Merrill *et al.*, Rev. Sci. Instrum. **83**, 10D317 (2012).
[17] H. W. Herrmann *et al.*, Rev. Sci. Instrum. **81**, 10D333 (2010).
[18] M. Gittings *et al.*, Comput. Sci. Discovery **1**, 015005 (2008).
[19] C. B. Yeamans, D. L. Bleuel, and L. A. Bernstein, Rev. Sci. Instrum. **83**, 10D315 (2012).
[20] R. Hatarik *et al.*, J. Appl. Phys. **118**, 184502 (2015).
[21] T. J. Murphy, Phys. Plasmas **21**, 072701 (2014).
[22] O. A. Hurricane *et al.*, Nature (London) **506**, 343 (2014).
[23] J. D. Schwarzkopf *et al.*, J. Turbul. **12**, N49 (2011).